IEEE Photonics Journal
An IEEE Photonics Society Publication

Open Access

Simultaneous Wavelength- and Mode-Division (De)multiplexing for High-Capacity On-Chip Data Transmission Link

Volume 8, Number 2, April 2016

Liangshun Han
Song Liang
Junjie Xu
Lijun Qiao
Hongliang Zhu
Wei Wang

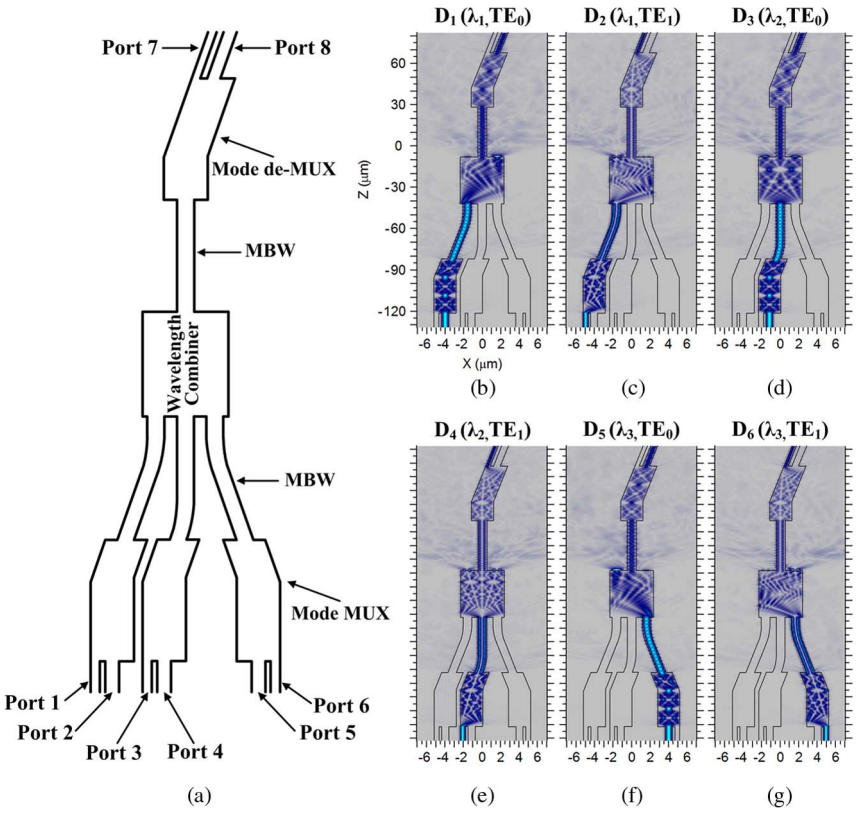

DOI: 10.1109/JPHOT.2016.2547419
1943-0655

Simultaneous Wavelength- and Mode-Division (De)multiplexing for High-Capacity On-Chip Data Transmission Link

Liangshun Han, Song Liang, Junjie Xu, Lijun Qiao, Hongliang Zhu, and Wei Wang

Key Laboratory of Semiconductor Materials Science, Institute of Semiconductors, Chinese Academy of Sciences, Beijing 100083, China

DOI: 10.1109/JPHOT.2016.2547419

Manuscript received February 5, 2016; revised March 18, 2016; accepted March 24, 2016. Date of publication March 28, 2016; date of current version April 12, 2016. This work was supported in part by the National High Technology Research and Development Program of China (863 Program) under Grant 2013AA014502 and Grant 2011AA010303; by the National Natural Science Foundation of China under Grant 61474112, Grant 61274071, Grant 61090392, and Grant 61006044; and by the National Basic Research Program of China (973 Program) under Grant 2012CB934202 and Grant 2014CB340102. Corresponding author: S. Liang (e-mail: liangsong@semi.ac.cn).

Abstract: We present designs of wavelength-division-multiplexing (WDM) and mode-division-multiplexing (MDM) optical links using mode de/multiplexers (DE/MUXs) based on multimode interference (MMI) couplers with a tilt joint as a phase shifter. The properties of WDM-MDM links with three wavelengths and two optical modes are numerically studied by using 3-D beam propagation method. In the first design, the wavelength combiner is also an MMI coupler type. The insertion loss of the design is around 6 dB because of the inherent loss of the MMI combiner. The size of the main passive optical parts (mode DE/MUXs and wavelength combiner) of the design is only $10.4 \times 114.2\ \mu m^2$, making the design promising for future compact and high-capacity optical interconnection applications. In another design, arrayed waveguide gratings are used for wavelength multiplexing, leading to a lower insertion loss of the optical connections. For both designs, the mode crosstalk between the two different modes for the same wavelength are below −22 dB.

Index Terms: Integrated optic devices, multiplexing, optical interconnects.

1. Introduction

On-chip optical interconnection is one of the most attractive schemes to meet the demands for high bandwidth and low power consumption of future massively paralleled microprocessors [1], [2]. A number of techniques have been studied to increase the capacity of the optical connections [3], [4]. A widely used way is wavelength division multiplexing (WDM) [5], [6], which enable higher speed of data transmission by transmitting multiple wavelengths on the same optical path. To further enlarge the communication bandwidth of the optical link, mode division multiplexing (MDM) has been proposed to be used in combination with the WDM. MDM provides a new dimension to increase the capacity of optical communications by using different guided modes as independent channels for transferring optical data. In recent years, WDM

interconnections compatible with MDM (WDM-MDM) has been presented by using different types of mode de/multiplexer (DE/MUX), which are based on asymmetrical directional couplers [7], [8] and asymmetrical Y-junctions, as well as adiabatic coupling [9], [10].

For MDM optical connections, high quality mode DE/MUX is one of the most important devices. We have recently proposed a novel mode DE/MUX based on MMI couplers, which has the advantages of compact size, low crosstalk, large optical bandwidth, and large fabrication tolerance [11]. In this paper, we present the designs of WDM-MDM link using the MMI-based DE/MUX. The mode crosstalk and loss of the proposed optical links are studied systematically. The results show that our links are promising for the future on-chip communications with ultra-high bandwidth.

2. Operation Principle and Structure Design

2.1. On-Chip WMDM-MDM Data Transmission Links

The schematic structures of two proposed WDM-MDM links are shown in Fig. 1. The links consist of transmitter (Tx) and receiver (Rx) modules which are connected by a multimode bus waveguide (MBW). In design A, the Tx module is composed of a multiple-wavelength laser array, a 1×2 power splitter array, a modulator array, a mode multiplexer (MUX) array, and a wavelength combiner. In the study, we consider only the transverse-electric (TE) polarized modes. The fundamental mode (TE_0) light beam from a single laser is split into two TE_0 parts with equal power by the 1×2 MMI-based power splitter. After being modulated by two modulators individually, one of the light beams is converted into the TE_0 mode of the output waveguide of the mode MUX, while the other is converted into the TE_1 mode. As a result, each wavelength can support two different data channels. Thus, the data channels can be listed as: $D_1(\lambda_1, \mathrm{TE}_0), D_2(\lambda_1, \mathrm{TE}_1), \ldots, D_{2N-1}(\lambda_N, \mathrm{TE}_0), D_{2N}(\lambda_N, \mathrm{TE}_1)$, where N is the wavelength number. All the TE_0 and TE_1 modes with different wavelengths are then collected by an MMI-based coupler into a single MBW. This coupler acts as both the wavelength and mode combiner and should be carefully designed to obtain consistent performance for all the different data channels. One advantage of the design is that the size of the Tx link can be extremely small because of the use of all MMI-based optical components.

The Rx module is used to demultiplex the different modes and wavelengths into photodetectors and comprises a two-mode demultiplexer (de-MUX), two AWGs, and a photodetector array. The data channels are first divided into two groups: the TE_0 group $D_1, D_3, D_5, \ldots$ and the TE_1 group $D_2, D_4, D_6, \ldots$ by our MMI-based two-mode de-MUX. At the same time, the TE_1 group has been converted into TE_0 mode and then both groups are collected by two output waveguides of the de-MUX, respectively. Two AWGs are then used to demultiplex the wavelength channels before they are fed to the photodetectors. In the proposed optical links, one of the challenges is to design a two-mode de-MUX with a large bandwidth.

An alternative design (design B) is shown in Fig. 1(b). In the Tx module, AWGs are used as the wavelength combiners. There are also laser arrays, 1×2 power splitter arrays, and mode multiplexer arrays. Though the arrangement of the lasers can be the same as that of design A, a different arrangement is shown in Fig. 1(b) so that crossing of the output waveguides of the 1×2 power splitters can be avoided. In the design, the lights from the lasers are split into two groups: $D_1, D_3, D_5, \ldots$ and the TE_1 group $D_2, D_4, D_6, \ldots$. After modulation, the different laser wavelengths in each group are multiplexed by two AWGs. The TE_0 outputs of the two AWGs, respectively, are converted to the TE_0 mode and the TE_1 mode of the MBW of the link. The Rx module of design B is the same as that of design A. The advantage of design B is that the inherent loss of the MMI-based wavelength combiner could be avoided because of the use of the AWG wavelength combiners.

As can be seen, the transmission capacity of the WDM-MDM link can be increased by simply adding more wavelengths. Higher order modes such as TE_2 or even TE_3 can also be adopted to further enlarge the capacity by using MMI-based DE/MUX with more complex structure [12].

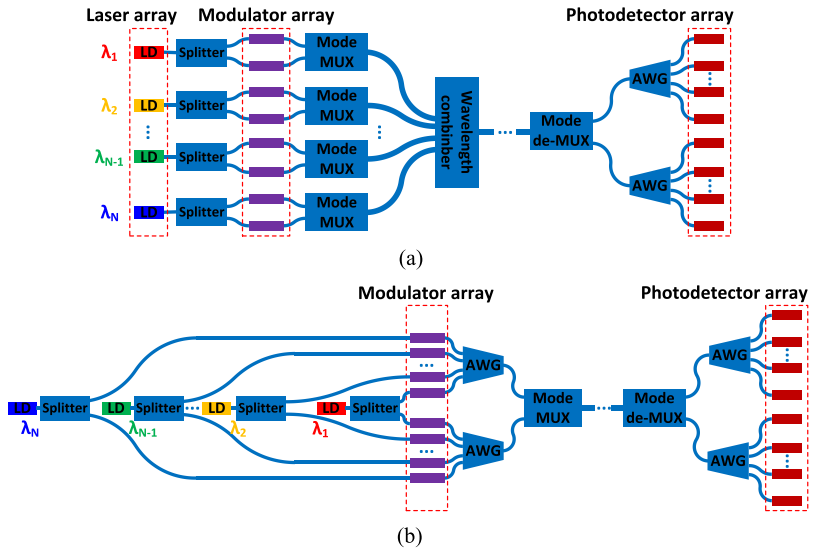

Fig. 1. Schematic structure of the WDM-MDM links. (a) Design A. (b) Design B. LD: laser diode.

The lasers can be readily integrated into link by different methods such as flip-chip [13] and selective area metal bonding technique [14]. Alternatively, the lights with different wavelengths can also be fed into the waveguides from fibers through grating couplers. To control the TE polarization of the light source, polarization beam splitter could also be integrated into the links to filter out transverse-magnetic modes.

To realize MDM optical communications, one essential component is mode DE/MUX. In this study, an MMI-based DE/MUX with a tilt joint as phase shifter is used [11]. It has been shown [11] that the MMI-based DE/MUX has the advantages of low loss, large fabrication tolerance, and relatively large optical bandwidth as compared with other types of mode DE/MUXs such as adiabatic couplers (ACs) [15], asymmetric *Y*-junctions [16]–[18], and asymmetrical directional couplers (ADCs) [19], [20].

2.2. MMI-Based Wavelength Combiner

In design A, an MMI coupler is used as the wavelength combiner, which combines the lights with different wavelengths in both TE_0 and TE_1 modes into a single MBW. As wavelength combiner, it is well known that the MMI couplers have a large optical bandwidth, which makes them suitable for WDM use as in this study. To be used for combining lights of different modes, the length of the MMI coupler needs to be optimized carefully. Fig. 2 shows the light field distributions in an MMI waveguide for TE_0 and TE_1 modes. For a symmetrical-interference-type MMI coupler, the self-imaging lengths are different for the TE_0 and TE_1 modes because of the different effective refractive index of the two modes. However, there are a number of lengths, such as L_1 and $L_2 = 2 \times L_1$ in the figure, where three-fold self-imaging can be realized for both the TE_0 and TE_1 modes at the same time. According to our simulations, the shortest length of the 3×1 MMI coupler with width of 4.8 μm which combines both the two modes simultaneously and efficiently is $L_1 = 35.0$ μm. Thus, the width and length of our MMI-based wavelength combiner is designed as 4.8 μm and 35 μm, respectively.

Fig. 3 shows the light field distribution in the 3×1 MMI combiner as the lights with the different modes are launched into the three input waveguides. As can be seen, all the lights can be collected by the output waveguide effectively, though there are light losses inherent to the MMI type combiner. The insertion losses of the different light channels as a function of the width of the combiner are shown in Fig. 4(a). As can be seen, including the inherent loss of the MMI combiner (about 4.77 dB), the insertion loss is less than 5.2 dB at the designed 4.8 μm width.

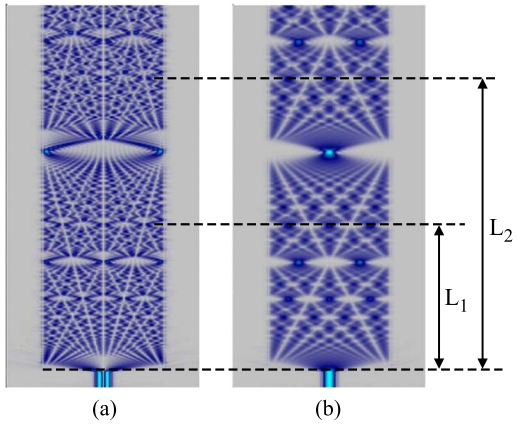

Fig. 2. Light field distributions in MMI waveguide for (a) TE_1 mode and (b) TE_0 mode.

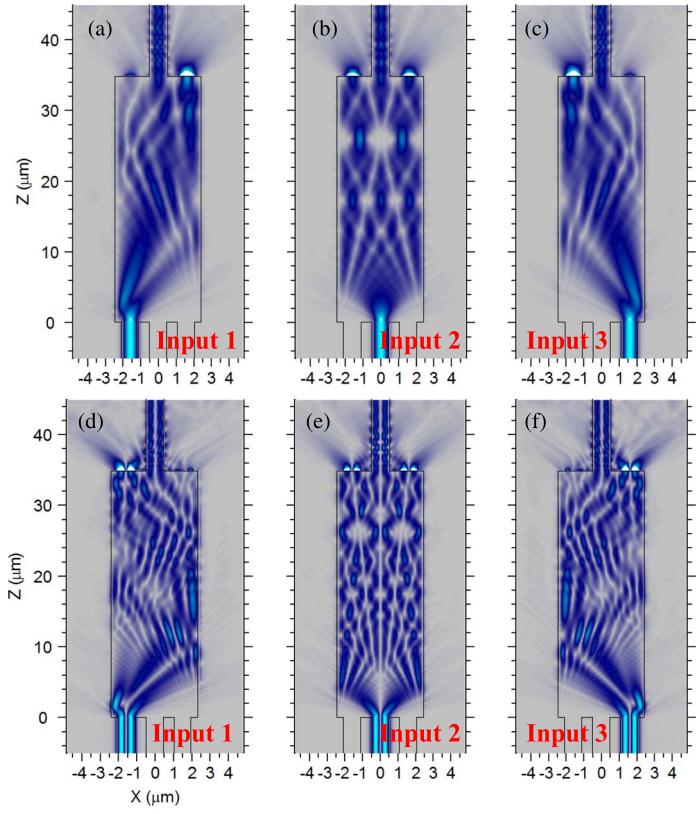

Fig. 3. Field distributions of the 3 × 1 MMI wavelength combiner when (a)–(c) TE_0 mode and (d)–(f) TE_1 mode are launched into Input 1 to Input 3.

As the MMI width is varied for ±20 nm, the loss is less than 5.5 dB. Even when the width variation is as large as ±35 nm, the loss is still smaller than 6.0 dB, which indicates a large fabrication tolerance of our combiner. Fig. 4(b) shows the insertion losses of the light channels as a function of the wavelength. It can be seen that the light loss is less than 6 dB within the wavelength range from 1520 nm to 1575 nm, which means that the MMI-based wavelength combiner possesses rather good wavelength insensitivity as other MMI-based devices.

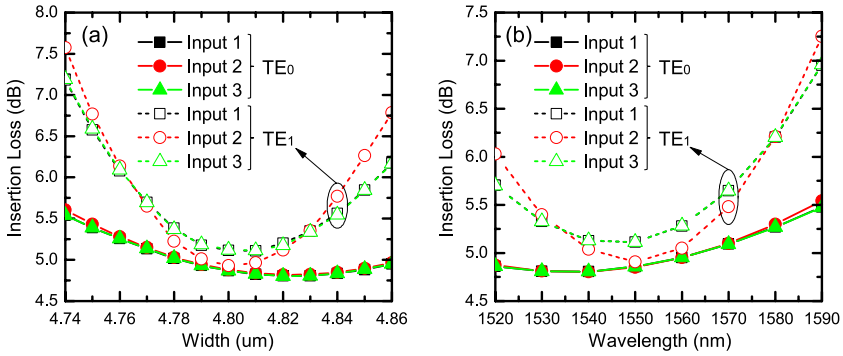

Fig. 4. Insertion losses of the different light channels as a function of (a) the width of the combiner and (b) the wavelength.

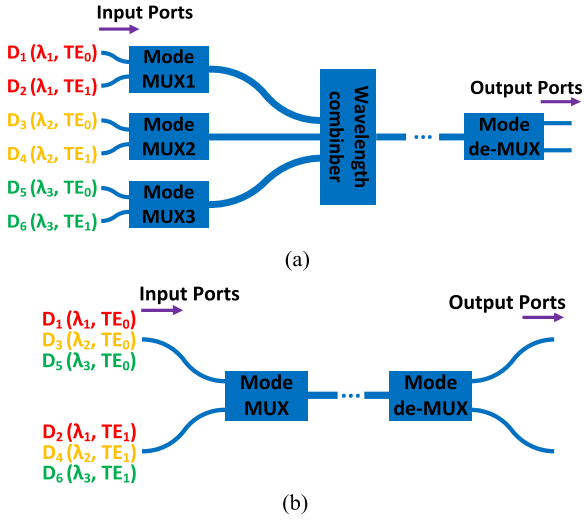

Fig. 5. Main passive optical parts related to MDM application (a) for design A and (b) for design B.

3. Simulation Results and Discussion

In this study, an SOI wafer with a 2 μm-thick silica insulator layer and a 250 nm silicon layer is considered as the fabrication platform. We used 3-D BPM [21] to evaluate the performance of the proposed optical links. The structure is covered with air. Because both the design and fabrication of the modulators, AWGs and photodetectors are rather mature on SOI wafer in nowadays, we focus only on the passive optical components related to realization of MDM function in this study, as shown in Fig. 5(a) and (b). As an example, here we discuss a WDM-MDM system with three wavelength channels having 3.0 nm channel spacing and two mode channels: TE_0 and TE_1. All the three wavelengths used in this study are $\lambda_1 = 1547$ nm, $\lambda_2 = 1550$ nm, and $\lambda_3 = 1553$ nm.

3.1. Design A

In design A, the two-mode de-MUX should be designed to possess a uniform performance for all the three wavelengths. Fortunately, large optical bandwidth is one of the advantages of MMI-based optical device. The bandwidth can be enlarged by increasing the width of MMI waveguide of the mode de-MUX though a large width leads to a longer device length. Although the three two-mode MUXs can be optimized individually according to the assigned wavelengths, to simplify the simulations, the MUXs are designed to have the same structure as the two-mode de-MUX in this study. The width of MMI coupler is set at 2.4 μm, and the corresponding

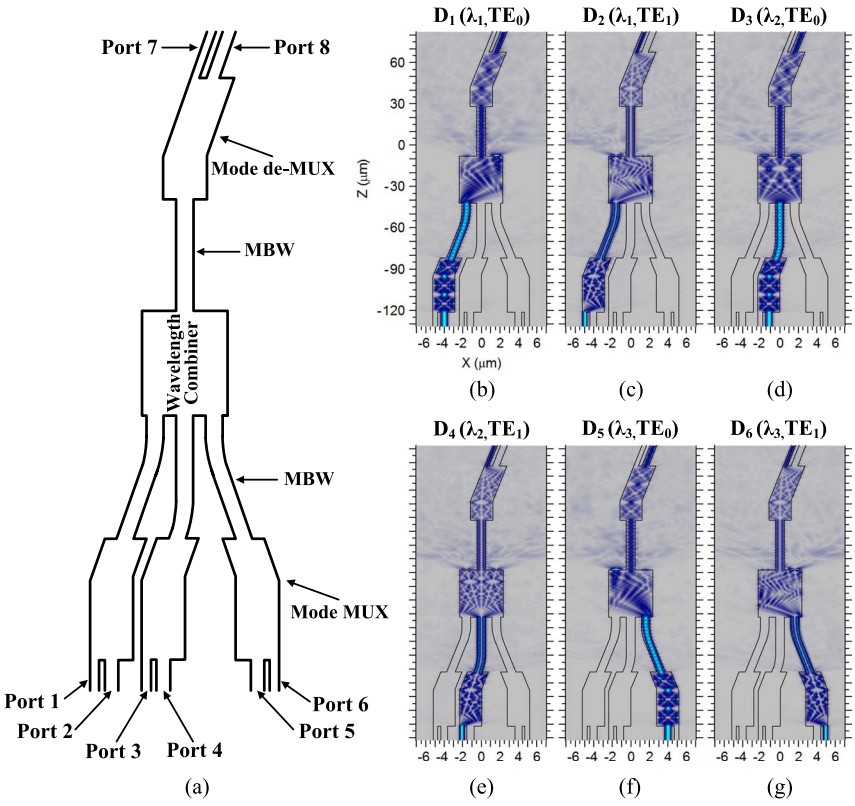

Fig. 6. (a) Layout of design A shown in Fig. 5(a). (b)–(g) Field distributions in this layout for different data channels.

TABLE 1

Parameters of each component in Fig. 6(a)

Component	Width (μm)	Tilt angle (deg.)	Length (μm)
MUX1	2.4 *	3.3	39.56
MUX2	2.4 *	3.3	39.56
MUX3	2.4 *	3.3	39.56
de-MUX	2.4 *	3.3	39.56
Wavelength Combiner	4.8 *	/	35.0
Port 1, Port 3, Port 6, and Port 7	0.53	/	/
Port 2, Port 4, Port 5, and Port 8	0.8	/	/
MBW	1.0	/	/

* The width is the MMI waveguide width of the component.

total length of this two-mode MUX is only 39.56 μm. The angle of the tilt joint in the MUX is 3.3 degree. As have been shown previously [11], the device has both a low de-multiplexing insertion loss and a low de-multiplexing crosstalk with the whole C band (1530 nm–1565 nm) wavelength range.

Fig. 6(a) shows the layout of the MDM passive parts in design A. The parameters of each component are given in Table 1. The widths of the single mode access waveguides (Port 1, Port 3, and Port 6) for outputting the TE_1 modes from the MUXs are set as 0.53 μm. The other three access waveguides for TE_0 modes have the same width of 0.8 μm. Three S-bend MBWs are used to connect the three two-mode MUXs with the MMI-based wavelength combiner. The width of these S-bend MBWs is 1.0 μm. The wavelength combiner, as designed above, is a 3 $\times$ 1 symmetrical-type interference coupler, whose width and length is 4.8 μm and 35 μm,

TABLE 2

Summary of the overall insertion losses of different data channels and crosstalk between modes with same wavelength in the link shown in Fig. 6(a). $\lambda_1 = 1547$ nm, $\lambda_2 = 1550$ nm, and $\lambda_3 = 1553$ nm

Data Channel	Insertion Loss (dB)	Mode Crosstalk (dB)
$D_1(\lambda_1, TE_0)$	5.11	-32.5
$D_2(\lambda_1, TE_1)$	6.30	-28.3
$D_3(\lambda_2, TE_0)$	5.23	-29.0
$D_4(\lambda_2, TE_1)$	5.85	-27.2
$D_5(\lambda_3, TE_0)$	5.45	-28.3
$D_6(\lambda_3, TE_1)$	6.14	-26.6

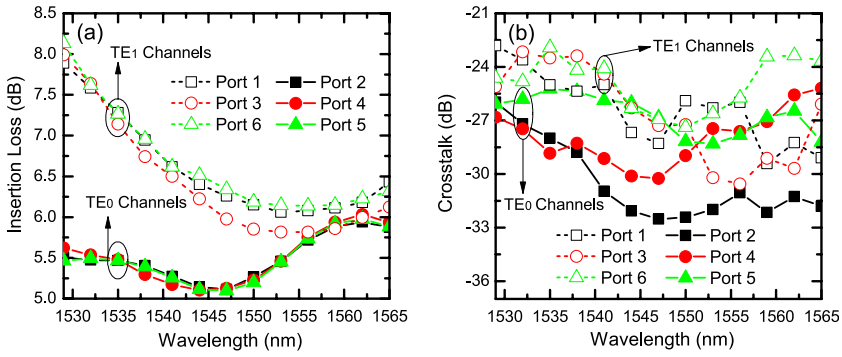

Fig. 7. Wavelength dependence of (a) insertion loss and (b) crosstalk of the link of different access waveguides shown in Fig. 6(a).

respectively. The output port of the wavelength combiner is a MBW, which is used to transmit all data channels to the Rx module. In the Rx module, we focus only on the two-mode de-MUX due to the mature design and fabrication of the silicon-based AWGs. The two-mode de-MUX has the same size and structure as the two-mode MUXs. Port 7 and Port 8 are used to collect TE_1 and TE_0 power as fundamental mode of the waveguides and have widths of 0.53 μm and 0.8 μm, respectively.

To demonstrate the transmission properties of the data channels, the simulated field distributions in the proposed data transmission link when lights with different wavelengths and modes are launched into the corresponding input ports are shown in Fig. 6(b)–(g). It is seen that the light powers of channels D_1, D_3, and D_5 are efficiently routed into Port 8 and the light powers of channels D_2, D_4, and D_6 are efficiently routed into Port 7, respectively, with less than 0.1 percent of the input power collected by the adjacent output ports for all the different channels. The insertion losses of the different data channels in this link are summarized in Table 2. During the whole mode and wavelength multiplexing and mode de-multiplexing processes, the overall insertion losses including inherent losses of the 3 $\times$ 1 MMI-based wavelength combiner and radiation losses of the S-bend waveguides are 5.11, 6.30, 5.23, 5.85, 5.45, and 6.14 dB, respectively. The insertion losses of each access waveguides of the link as a function of wavelength are shown in Fig. 7(a). The light loss is less than 8.2 dB within the wavelength range from 1529 nm to 1565 nm with 3 nm step. In practice, every MUX can be optimized for the assigned wavelength to obtain better performance. Because the crosstalk among the different wavelengths depends on the performance of AWGs, we only evaluate the crosstalk between the TE_0 and TE_1 modes having the same wavelength, which are –32.5, –28.3, –29.0, –27.2, –28.3, and –26.6 dB, respectively, as also shown in Table 2. The mode crosstalk of each access waveguides of the link as a function of wavelength are shown in Fig. 7(b). As can be seen, the cross talk is better than –22.8 dB within the wavelength range from 1529 nm to 1565 nm.

Because of the MMI wavelength combiner, the insertion loss for the three wavelength system is around 6 dB, which is larger than the loss of the WDM-MDM system realized by other

TABLE 3

Parameters of each component in Fig. 8(a)

Component	Width (μm)	Tilt angle (deg.)	Length (μm)
MUX	2.4 *	3.3	39.56
de-MUX	2.4 *	3.3	39.56
Port1 and Port 3	0.53	/	/
Port2 and Port 4	0.8	/	/
Multimode Bus Waveguide	1.0	/	/

* The width is the MMI waveguide width of the component.

techniques [7], [9]. However, due to the MMI-based optical components used, the size of the mode and wavelength MUX in Fig. 5(a) is only $10.4 \times 114.2\ \mu m^2$ (does not include the output MBW of the wavelength combiner and the input waveguides of the mode MUXs). Comparatively, the length of the Y-junction based mode MUX device is as large as 1200 μm in reference [9]. In another work [7], the mode MUXs are based on as asymmetrical directional couplers (ADCs), which can have smaller sizes. However, the on chip wavelength (de)multiplexer based on AWGs have large width and length, which are both hundreds of microns. The small size of our mode and wavelength MUX makes it a promising candidate for future compact and high-capacity optical interconnection applications.

3.2. Design B

As shown in Fig. 1(b), in the design, two AWGs are used to multiplex the different wavelengths before modes multiplexing. Unlike in design A, only a single two-mode MUX is employed to realize the two modes multiplexing for the three wavelengths. A two-mode de-MUX having the same structure as the MUX device is used for demultiplexing the two modes. Table 3 gives the parameters of the optical components of this design. Fig. 8 shows the layout and simulated field distributions in design B when different wavelengths are launched. Similar as in design A, the wavelength multiplexing and demultiplexing losses and crosstalk depend on the AWGs. As summarized in Table 4, the insertion losses of different data channels and crosstalk between modes having the same wavelength for data channel form D_1 to D_6 are 0.37, 0.99, 0.36, 0.96, 0.36, 1.0 dB, and –24.3, –32.0, –25.5, –34.3, –26.9, –31.2 dB, respectively. The sizes of both the mode MUX and the whole links as shown in Fig. 1(b) (lasers and detectors not included) are comparable to those reported in reference [7], where ADCs are used as mode DE/MUX and AWGs are used as on chip wavelength demultiplexer. The insertion loss of the design is also similar to the work counting the excess loss of the fabricated AWGs [7].

It should be noted that the capacity of the proposed link can be expanded by using more channels of both the wavelength and mode. By a cascading structure, the MMI-based mode DE/MUXs can be extended to more than two modes [12]. By using an $N \times 1$ wavelength combiner, where $N > 3$, more wavelengths can be used. For design A, more wavelengths would increase the insertion loss of the system. Thus, the design is more suitable for WDM-MDM optical link with a small number of wavelength channels. However, the advantage of design A is that both the design and fabrication of the MMI-based wavelength optical components are relatively easy. What's more, the size of the Tx module of the design is a lot smaller than ones that need AWG for wavelength multiplexing. Then, more wafer space can be used for the fabrication of other optical or electrical devices, helping to enhance the performance of the whole chip. For the case of having a large number of wavelength channels design B is more suitable because of the low insertion loss of AWGs. Although, in this study, channels with a 3 nm spacing channel are used to demonstrate the properties of the optical link, wavelengths with smaller channel spacing, such as 0.4 nm, 0.8 nm, and 1.6 nm, can be adopted to increase the spectrum efficiency.

It is well known that MMI couplers can suffer from reflections when some light is imaged outside the output waveguides [22]. As shown in Figs. 3 and 6, it is obvious that some light power

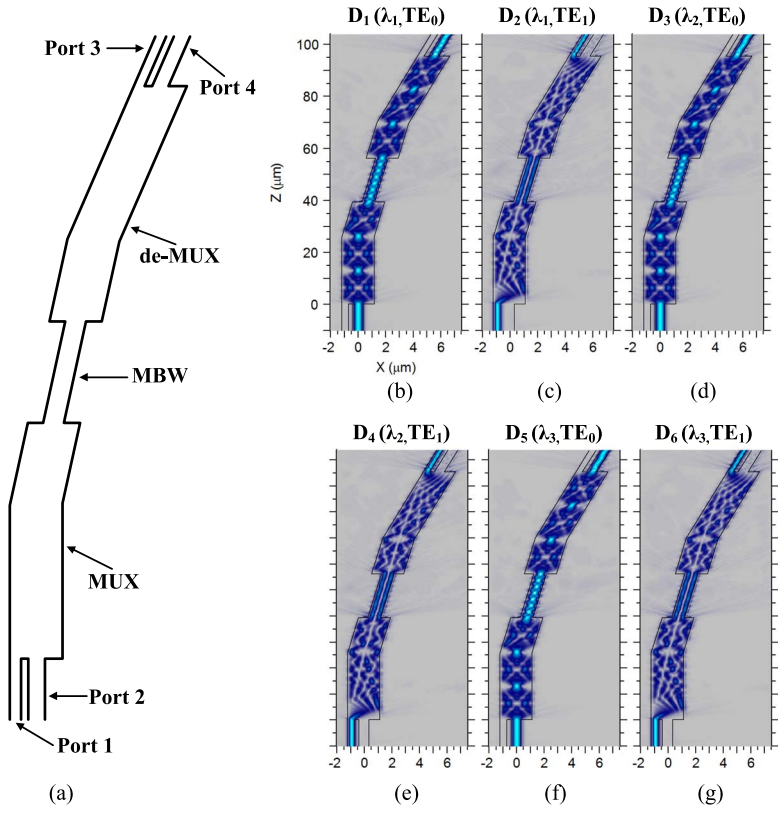

Fig. 8. (a) Layout of design B shown in Fig. 5(b). (b)–(g) Field distributions in this layout for different data channels.

TABLE 4

Summary of the overall insertion losses of different data channels and crosstalk between modes with same wavelength in the link shown in Fig. 8(a). $\lambda_1 = 1547$ nm, $\lambda_2 = 1550$ nm, and $\lambda_3 = 1553$ nm

Data Channel	Insertion Loss (dB)	Mode Crosstalk (dB)
$D_1(\lambda_1, TE_0)$	0.37	-24.3
$D_2(\lambda_1, TE_1)$	0.99	-32.0
$D_3(\lambda_2, TE_0)$	0.36	-25.5
$D_4(\lambda_2, TE_1)$	0.96	-34.3
$D_5(\lambda_3, TE_0)$	0.36	-26.9
$D_6(\lambda_3, TE_1)$	1.0	-31.2

is outside the MBW at the exit facets of MMI coupler of the wavelength combiner, which would case back-reflected light due to the discontinuous refractive index. The effects of the remaining light reflections on the crosstalk values should be small, because the light is reflected backward and is then further reflected and attenuated for may be several times by the edges of the MMI couplers before being able to be coupled into the output waveguides. What's more, several methods have been proposed to further reduce the reflection level of MMI-based combiner, such as loss waveguide [23], low refractive index contrast access waveguides [24], and tilted exit facets [25].

4. Conclusion

We present designs of WDM-MDM optical interconnections using mode DE/MUXs based on multimode interference couplers with a tilt joint as phase shifter. In one design, the wavelength

combiner is also an MMI coupler type. The insertion loss of the design is relatively large because of the inherent loss of the MMI combiner. However, the Tx module of the design has a very small size, making the design promising for future compact and high-capacity optical interconnection applications. In another design, AWGs are used for wavelength multiplexing, leading to a lower insertion loss of the optical connections. The design is more fit for the case having a large number of wavelength channels. For both the two designs, the mode crosstalk between the two different modes for the same wavelength are rather low.

References

[1] K. Ohashi *et al.*, "On-chip optical interconnect," *Proc. IEEE*, vol. 97, no. 7, pp. 1186–1198, Jul. 2009.
[2] A. Shacham, K. Bergman, and L. P. Carloni, "Photonic networks-on-chip for future generations of chip multiprocessors," *IEEE Trans. Comput.*, vol. 57, no. 9, pp. 1246–1260, Sep. 2008.
[3] D. Qian *et al.*, "101.7-Tb/s (370 × 294-Gb/s) PDM-128QAM-OFDM transmission over 3 × 55-km SSMF using pilot-based phase noise mitigation," in *Proc. Opt. Fiber Commun. Conf./Nat. Fiber Opt. Eng. Conf.*, Los Angeles, CA, USA, 2011, pp. 1–3.
[4] A. Sano *et al.*, "69.1-Tb/s (432 × 171-Gb/s) C- and extended L-band transmission over 240 km using PDM-16-QAM modulation and digital coherent detection," in *Proc. Opt. Fiber Commun. Conf./Nat. Fiber Opt. Eng. Conf.*, San Diego, CA, USA, 2010, pp. 1–3.
[5] B. Jalali and S. Fathpour, "Silicon photonics," *J. Lightw. Technol.*, vol. 24, no. 12, pp. 4600–4615, 2006.
[6] R. Nagarajan *et al.*, "Large-scale photonic integrated circuits," *IEEE J. Sel. Topics Quantum Electron.*, vol. 11, no. 1, pp. 50–65, Jan./Feb. 2005.
[7] J. Wang, S. Chen, and D. Dai, "Silicon hybrid demultiplexer with 64 channels for wavelength/mode-division multiplexed on-chip optical interconnects," *Opt. Lett.*, vol. 39, no. 24, pp. 6993–6996, Dec. 15, 2014.
[8] Y. D. Yang, Y. Li, Y. Z. Huang, and A. W. Poon, "Silicon nitride three-mode division multiplexing and wavelength-division multiplexing using asymmetrical directional couplers and microring resonators," *Opt. Exp.*, vol. 22, no. 18, pp. 22172–83, Sep. 8, 2014.
[9] J. B. Driscoll *et al.*, "A 60 Gb/s MDM-WDM Si photonic link with < 0.7 dB power penalty per channel," *Opt. Exp.*, vol. 22, no. 15, pp. 18543–18555, Jul. 28, 2014.
[10] N. Riesen, J. D. Love, and J. W. Arkwright, "Few-mode elliptical-core fiber data transmission," *IEEE Photon. Technol. Lett.*, vol. 24, no. 5, pp. 344–346, Mar. 2012.
[11] L. Han *et al.*, "Two-mode de/multiplexer based on multimode interference couplers with a tilted joint as phase shifter," *Opt. Lett.*, vol. 40, no. 4, pp. 518–21, Feb. 15, 2015.
[12] Y. Kawaguchi and K. Tsutsumi, "Mode multiplexing and demultiplexing devices using multimode interference couplers," *Electron. Lett.*, vol. 38, no. 25, pp. 1701–1702, 2002.
[13] T. Mitze *et al.*, "CWDM transmitter module based on hybrid integration," *IEEE J. Sel. Topics Quant. Electron.*, vol. 12, no. 5, pp. 983–987, Sep./Oct. 2006.
[14] L. Tao *et al.*, "4-lambda InGaAsP-Si distributed feedback evanescent lasers with varying silicon waveguide width," *Opt. Exp.*, vol. 22, no. 5, pp. 5448–5454, Mar. 10, 2014.
[15] N. Riesen and J. D. Love, "Tapered velocity mode-selective couplers," *J. Lightw. Technol.*, vol. 31, no. 13, pp. 2163–2169, Jul. 2013.
[16] W. Chen, P. Wang, and J. Yang, "Mode multi/demultiplexer based on cascaded asymmetric Y-junctions," *Opt. Exp.*, vol. 21, no. 21, pp. 25113–25119, Oct. 21, 2013.
[17] J. B. Driscoll *et al.*, "Asymmetric Y junctions in silicon waveguides for on-chip mode-division multiplexing," *Opt. Lett.*, vol. 38, no. 11, pp. 1854–1856, Jun. 1, 2013.
[18] J. D. Love and N. Riesen, "Single-, Few-, and multimode Y-junctions," *J. Lightw. Technol.*, vol. 30, no. 3, pp. 304–309, 2012.
[19] M. Greenberg and M. Orenstein, "Multimode add-drop multiplexing by adiabatic linearly tapered coupling," *Opt. Exp.*, vol. 13, no. 23, p. 9381, 2005.
[20] Y. Ding *et al.*, "On-chip two-mode division multiplexing using tapered directional coupler-based mode multiplexer and demultiplexer," *Opt. Exp.*, vol. 21, no. 8, pp. 10376–10382, Apr. 22, 2013.
[21] J. Yamauchi, J. Shibayama, O. Saito, O. Uchiyama, and H. Nakano, "Improved finite-difference beam-propagation method based on the generalized Douglas scheme and its application to semivectorial analysis," *J. Lightw. Technol.*, vol. 14, no. 10, pp. 2401–2406, 1996.
[22] Y. Gottesman, E. V. K. Rao, D. Piot, E. Vergnol, and B. Dagens, "An in-depth analysis of reflections in MMI couplers using optical low-coherence reflectometry: Design optimization and performance evaluation," *Appl. Phys. B*, vol. 73, no. 5, pp. 609–612, Oct. 2001.
[23] Y. Gottesman, E. V. K. Rao, and B. Dagens, "A novel design proposal to minimize reflections in deep-ridge multimode interference couplers," *IEEE Photon. Technol. Lett.*, vol. 12, no. 12, pp. 1662–1664, Dec. 2000.
[24] Y. Li and R. Baets, "Improved multi-mode interferometers (MMIs) on silicon-on-insulator with the optimized return loss and isolation," in *Proc. IEEE 16th Annu. Symp. Photon. Benelux Chapter*, 2011, pp. 205–208.
[25] E. Kleijn *et al.*, "Multimode interference couplers with reduced parasitic reflections," *IEEE Photon. Technol. Lett.*, vol. 26, no. 4, pp. 408–410, Feb. 2014.